

Analysing lead carriers and examining their efficiency and properties in relation to dark matter studies using Accelerator Mass Spectrometry

Pranav Pativada u7286976 1st Year

ABSTRACT: Lead-210 (^{210}Pb) is a key radioimpurity that affects the SABRE (Sodium-Iodide with Active Background REjection) experiment's ability to precisely measure the claimed annual modulation caused for dark matter studies. Characterising ^{210}Pb is crucial as it releases low energy background events sensitive to this modulation range. PbF_2 mixed primarily with AgF_2 will be examined in terms of Pb ion output, efficiency and degradation over time. Several Pb compounds were prepared for ^{210}Pb and ^{208}Pb detection using AMS (Accelerator Mass Spectrometry) to determine which Pb material had the lowest $^{210}\text{Pb}/^{208}\text{Pb}$ isotopic ratio. Procedures involved chemical preparation of carriers and AMS beam time. Results indicate that unpurified carriers had lower $^{210}\text{Pb}/^{208}\text{Pb}$ isotopic ratios compared to the purified ones. Samples of $\text{PbF}_2 + \text{AgF}_2$ were unpredictable as an AMS target but yielded adequate current outputs. A beam efficiency of 0.081% was calculated. Inconclusive results were obtained from degradation and more time was needed to see noticeable change. Future work would involve new methods for purification, alternate ways to create Pb carrier samples, and optimization of AMS procedures that would help with further characterising ^{210}Pb .

1. INTRODUCTION

Experimental observations from a myriad of astrophysical techniques have inferred the existence of Dark Matter (DM). DM is responsible for many conjectures of the Universe - primarily the galaxy rotation curve [1]. The nature of DM has been attributed to many hypotheses, with the leading candidate being WIMPs (Weakly Interacting Massive Particles) scattered in a galactic halo [2].

The WIMP-DM scenario is where our galaxy is surrounded by a spherical WIMP halo consisting of WIMPs with isotropic velocities [3] [4]. The motion of these WIMPs in combination with that of our galaxy and the Earth results in rare WIMP-nuclear collisions with matter. These collisions produce a nuclear recoil in the form of low-energy scintillation light that is able to be detected. The rate of WIMP nuclear collisions ensue an annual modulation due to Earth's orbital motion [2][5]. In reference to the halo frame, the Earth's speed changes as it orbits the Sun which modulates these interactions on an annual basis [3].

Evidence that supports the WIMP-DM scenario through a long-standing observed annual

modulation has been found through DAMA (DArk MAtter) experiment. The DAMA experiment, which originally began as DAMA/NaI and then remodelled as DAMA/LIBRA (LIBRA standing for Large sodium Iodide Block for RAre Processes), aimed to detect WIMPs through direct measurement - a technique that observes the aforementioned low-energy recoils in a laboratory environment [2][6]. Through the use of highly sensitive radiopure and ULB (Ultra Low Background) NaI(Tl) crystal scintillators, WIMP-crystal interactions releasing energies would be detected [7]. Throughout a 26 year span and totalling 22 annual cycles from the combination of DAMA/NaI and DAMA/LIBRA observations with distinct phases, an annual modulation of $0.01014 \pm 0.00074 \text{ cpd/kg/keV}$ was recorded over a 2 - 6 keV energy range with a high statistical significance of 13.7σ , meaning that it is compelling evidence for the WIMP-DM scenario [8][9].

However, this evidence has not been replicated yet. Instead, other experiments have found contradictory evidence in this energy range [7]. As such, skepticism has risen about the results of the DAMA experiment. Criticisms are that the modulation is due to on-site and seasonal effects

that have nothing to do with WIMPs. Examples of such are annual humidity fluctuations, indirect sunlight and cosmic muon effects, and temperature swings.

The SABRE experiment aims to replicate the results from DAMA. To account for the criticisms, SABRE has planned to conduct two experiments, one in each hemisphere - SABRE North and SABRE South [5]. These dual sites can identify whether the modulation is due to on-site or seasonal effects thanks to the experiments being in different locations and a phase inversion between the hemispheres[2]. Utilising the same techniques, SABRE has grown NaI(Tl) crystals with a background rate of 0.01 cpd/kg/keV - the most radiopure crystals to date and seven times lower than that of DAMA [7].

Despite these improvements, intrinsic radioisotopes that release energy in the modulation range are fundamental limitations for SABRE as they can often be indistinguishable from actual WIMP-related events. The characterisation of radioimpurities and their behaviours that cause these background events is essential. ^{40}K , ^{238}U , ^{232}Th , ^{87}Rb and ^{210}Pb are amongst the key radioimpurities that affect SABRE's sensitivity [7]. SABRE's efforts to produce the purest crystals have minimised contributions from ^{40}K , ^{238}U , ^{232}Th and ^{87}Rb . Using a technique called ICP-MS (Inductively Coupled Plasma Mass Spectroscopy) that measures the background environment, these radioimpurities range from 4.7 ppb to well under 1 ppt - much less than the DAMA counterpart [5][7]. This leaves ^{210}Pb to be characterised. Due to low concentrations of ^{210}Pb in the environment, ICP-MS cannot be used for background detection. ^{210}Pb can only be measured by direct counting techniques - such as AMS [7].

The purpose of this project is to use AMS techniques to characterise the behaviour of ^{210}Pb . This will be done by preparing different Pb carrier samples. A Pb carrier acts chemically the same as ^{210}Pb , so its properties can be analysed to the likes of ^{210}Pb [10]. These samples will be bombarded with cations such as Cs^+ to be ionised in AMS. An injection magnet will then filter out the target ions that needs to be measured. They are then detected via a measure of current through a Faraday cup. This process is

illustrated in Figure 1. A higher and more stable current output leads to better sample efficiency as more extracted material is detected. This can be used to calculate the presence of an isotope in a sample, as with ^{210}Pb . Carrier samples will be made from a Pb roof, shielding material, and a combination of Pb compounds. These will be made for 3 distinct purposes as follows.

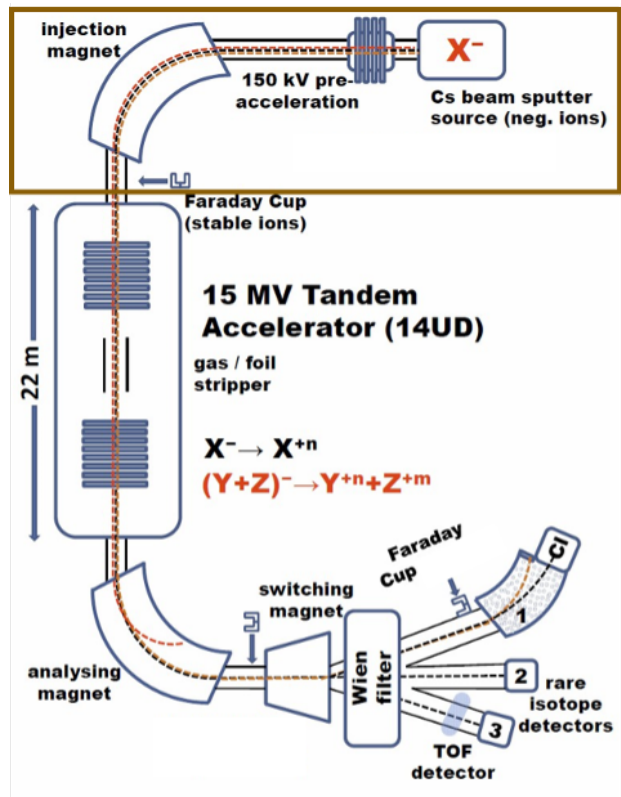


Figure 1: Schematics of the 14UD Heavy Ion Accelerator at the Australian National University. Only the top part that is outlined will be used.

1.1 Carrier Purity

Carrier purity of samples can affect the amount of ^{210}Pb to ^{208}Pb . Minimising the amount of ^{210}Pb is key as it reduces the amount of background events by ^{210}Pb . To test this, two sets of samples; one conventional and the other purified, will be made. The conventional set will be carrier samples that will go through a fluorination process as the AMS target material is PbF_2 . The purified set will go through column chromatography to remove any potential impurities, and then fluorination. It is hypothesised that the purified sample set will have a better current output as there are less impurities, leading to more material being extracted.

1.2 Carrier Efficiency

Past experimental procedures with ^{210}Pb detection have recorded success with PbF_2 as an AMS target sample for current output. Mixtures of PbF_2 with Ag, AgF and AgF_2 will be prepared for identifying which gives the highest and most stable current output, with emphasis on AgF_2 . AgF_2 was chosen because it is a so-called fluorinating agent, meaning it might act as a stronger fluorine donor than PbF_2 , forcing PbF_2 to accept an F atom and be able to extract PbF_3^- from the AMS target material. Samples will go through AMS at the HIAF (Heavy Ion Accelerator Facility) at ANU (Australian National University). It is hypothesised that the PbF_2 and AgF_2 sample will yield the best current output as AgF_2 contains two fluorine atoms compared to Ag and AgF .

1.3 Degradation Effects

The primary material being used is PbF_2 . PbF_2 absorbs moisture and this can decrease its efficiency when measured in AMS [10]. As sample preparation cannot be instantaneous for AMS and samples are exposed to air, they degrade over time. Six degradation samples of $\text{PbF}_2 + \text{AgF}_2$ and $\text{PbF}_2 + \text{SbF}_3$, both with ratios of 1:2 (ideally 2.5 mg: 5.0 mg), were prepared in cathodes of the Cu, Al and SS (Stainless Steel) in N_2 and air environments. This will aim to test how much exposure and time is needed for PbF_2 before it is effectively useless.

2. METHODOLOGY

2.1 Carrier Purity Procedures

2.1.1 Initial Chemical Preparations

0.2077 g of PbF_2 was weighed and then transferred to a ceramic crucible to dry at 100°C via a muffle furnace. This PbF_2 will be used for the experiments detailed in 1.1, 1.2 and 1.3. Two slices of shielding material, the top right (Pb_20002) and the top left (Pb_20003) were placed in separate beakers for acid leaching. 2.5 mL of IQ sub-boiled 67% - 69% HNO_3 was added, and swirled. These were put into an ultrasonic bath for 1-2 minutes, and the solutions were transferred into

two separate centrifuge tubes. High-resistance 18.2Ω MQ water (MQ water) was used to collect the residue. This was then transferred, and the process was repeated twice more.

This acid leaching process was to clean the material and gather up the surface impurities. It was also used to decompose some of the Pb material into solution so it could be used as a carrier sample.

Two Teflon vials were weighed. The Pb_20002 and Pb_20003 beakers were sprayed with MQ water and swirled, and then 2.5 mL of the solution was transferred to the teflon vials. This was repeated twice more.

PbO_2 was weighed: 10.1 mg (PbO_2_1) and 13.7 mg (PbO_2_2) into two new Teflon vials. For PbF_2 , 10mg (PbF_2_1) and 11.3 mg (PbF_2_2) was weighed.

2.1.2 _1 Sample Preparations

100 μL 48% HF was added to the "_1" samples in intervals of a few hours. After addition, these were put into the heating block. This was an ongoing process that lasted a few days. During this process, 10mL of 1.5 M HCl to Pb_20002 and Pb_20003 was mistakenly added. As these have already reacted with HF, this potentially removes the effect of the fluorination process. Further HF needs to be added.

All "_1" samples were taken out and left to cool. Two sets (a /A and a /B set) were then pressed. This involved mixing the sample with Ag powder (99.999% metal basis Alfa Aesar) in a 1:2 mass ratio of ideally 2.5 mg of the sample with 5.0 mg of Ag. Table 1 shows the _1 samples and their masses.

"_1" Sample Masses ($\pm 0.05\text{mg}$)		
Sample Name	PbF_2 (mg)	Ag (mg)
$\text{Pb}_\text{20002.1/A}$	2.6	5.4
$\text{Pb}_\text{20002.1/B}$	2.5	4.6
$\text{Pb}_\text{20003.1/A}$	2.7	5.5
$\text{Pb}_\text{20003.1/B}$	2.7	5.5
$\text{PbO}_2_\text{1/A}$	2.7	6.0
$\text{PbO}_2_\text{1/B}$	2.3	4.4
$\text{PbF}_2_\text{1/A}$	2.6	5.2
$\text{PbF}_2_\text{1/B}$	2.4	4.6

Table 1: _1 sample masses that were pressed. uncertainties of ± 0.05 mg

2.1.3 _2 Sample Preparations

To all ”_2” samples, 0.5 mL of 30% Superpure® UTEVA HCl was added and placed into the heating block till the reaction subsided. This was repeated twice. For column chromatography, 1.5g per sample of E Resin (Anionic Exchange Resin - Cl Form) was weighed in a 25 mL beaker, then filled two-thirds with MQ water, swirled and decanted. The decanting process was repeated twice with around 2 hour intervals in between. 1.5M and 0.05M HCl dilutions were prepared and 5 columns were set up.

Equal amounts of AE Resin was transferred into the 5 columns. The resin height was 3.5cm, shorter than the expected 5cm. This meant the possibility of the lead being removed with the impurities and not being retained onto the resin. The resin was conditioned with 1.5mL of 1.5M HCl. 10 mL of 1.5M HCl was added to all four ”_2” samples, then stirred. This was repeated once.

Four centrifuge tubes were weighed separately, then each sample was transferred, and then re-weighed. These were placed into the centrifuge machine to ensure that the rest of the material that didn’t dissolve would not go through the resin. After being centrifuged, all four ”_2” samples were loaded onto their columns. 15mL of 1.5M HCl was added to the 5th column. This was the chemical blank that acted as a control and tested for cross-contamination. After the initial samples were eluted, 35mL of 1.5M HCl was added to all. To elute Pb, 40mL of 0.05M HCl was added to all samples. After Pb elution, the Pb fractions were put into the heating block for evaporation and were left overnight.

Observations of _2 samples show that there was almost no mass after evaporation. All samples were the size of a spock, similar to that of a blank. A possibility was that due to the decreased height of the resin, the Pb was eluted with the Fe. Therefore, the Fe fractions were evaporated and column chromatography was repeated.

It was observed that the Pb was indeed in the Fe fraction. Each ”_2” sample was transferred and dried at 100°C. Afterwards, these were pressed similar to the _1 samples. Then alongside the _1 samples, these were sent to ANSTO (Australian Nuclear Science and Technology Organisation) for AMS. Table shows the _2 sample masses.

2.2 Carrier Efficiency Procedures

2.2.1 $PbF_2 + AgF_2$ Sample Preparations

PbF_2 and AgF_2 (Sigma Aldrich AgF_2) with respective mass ratios of 7.3:7:6, 7:4:15.1, 3.0:15.3

”_2” Sample Masses ($\pm 0.05mg$)		
Sample Name	PbF2 (mg)	Ag (mg)
Pb_20002_2/A	2.4	5.3
Pb_20002_2/B	2.6	4.9
Pb_20003_2/A	2.4	4.9
Pb_20003_2/B	2.6	4.7
PbO2_2/A	2.4	5.0
PbO2_2/B	2.5	5.1
PbF2_2/A	2.3	4.9
PbF2_2/B	2.5	4.8

Table 2: _2 sample masses that were pressed

and 3.0:30.3 were weighed out (in mg) and transferred into Teflon vials. Then, 100 μL of 48% HF was added to all and these were put into the heating block. The samples were then transferred into ceramic crucibles to dry at 100°C. Two samples were pressed for each of the ratios of 1:1, 1:2, 1:5 and 1:10. Samples of PbF_2 mixed with Ag and AgF in these ratios were pressed as well by M. Webber and A. Chan.

The 1:5 and 1:10 samples were still moist regardless of being in the muffle furnace for a long time. These were put back in for drying. They were then transferred to weighing paper. The 1:5 was dry, but the 1:10 was not. The 1:10 sample was put on a hot plate, however this resulted in the sample being burnt out and infused with some weighing paper. The 1:5 was pressed, and the leftovers of the 1:10 was pressed.

2.2.2 AMS Beam Time

AMS process was begun using an Fe_2O_3 sample to test the beam as there is past experimental data suggesting an expected beam current of 2nA for $^{56}FeO^-$. This was done by determining the magnetic field for $^{56}Fe^{16}O$, then measuring the current output for $^{56}Fe^{16}O$ and $^{54}Fe^{16}O$ and finding the ratio to see if it matches up with the abundance ratio. The magnetic field strength to calculate PbF_3^- was found through scaling the current field strength (B_1) with the ratio of the current ion species mass (m_1) and the target mass (m_2) via the relationship: B_2

$= B_1 \times \sqrt{\frac{m_1}{m_2}}$. The target sample was set to $\text{PbF}_2\text{-}1$. Starting from the PbF_3^- magnetic field of 11165.9G, the magnetic field was incrementally scaled down to 9845G to detect the different ion species and their field strengths. This was done when there was a sudden peak in the beam current. The ion species observed at each peak was cross referenced with the above relationship and then the ratio between the currents was taken to check with the Pb abundance ratios. While most were in agreement, ^{206}Pb and ^{207}Pb yielded higher currents than expected as the $^{206}\text{Pb}/^{208}\text{Pb}$ and $^{207}\text{Pb}/^{208}\text{Pb}$ ratios were over 38% compared to the abundance ratios. This is because there were other clusters and compounds that were detected alongside ^{206}Pb and ^{207}Pb .

However, this is unproblematic as $^{208}\text{PbF}_3^-$ was selected to be the AMS target measurement and that had a higher current output. This was confirmed as a 1:5 sample from PbF_2+Ag , PbF_2+AgF , $\text{PbF}_2+\text{AgF}_2$ was scanned through and PbF_3^- was the most prolific.

A loop initialisation was performed to calculate the length of a loop. A loop was 32.3 seconds - consisting of two sets of around 10 second measurement time and 6 seconds swapping time. During measurements, the following were adjusted; tuning, ioniser and current scale.

- Ioniser: Controls how much Cs^+ the sample is bombarded by.
- Tuning: Focuses and optimizes beam current.
- Current Scale: The scales used were 2 μA , 600 nA, 200 nA, 60 nA, 20 nA, 6 nA and 2nA. The initial scale was first set, and then these were switched depending on the current output and were changed between loops so measurements were unaffected.

Samples were measured for 2000s (62 loops) one after the other. This began with measuring each ratio from each sample (the /A sample was usually measured unless already used by the 1:5 measurement before). Then, the 1:1, 1:2 and 1:10 samples for $\text{PbF}_2+\text{AgF}_2$ were measured. This is because the /A versions were consumed quickly and almost no current was observed. The /B samples were to check whether this was the case again, as the either the accelerator had a problem or the sample was bad.

Sample 11 (PbF_2+Ag 1:10-1) was measured

once more, and after other samples were measured, it was measured 5 times again. This was to calculate the beam efficiency. This sample was chosen as past experimental data has used PbF_2+Ag and there is a lower percentage of PbF_2 in the sample. Since we want to minimise ^{210}Pb due to contamination, this sample would contain less. Table 3 shows the samples that were pressed in 2.2.1 as well as the Fe_2O_3 sample.

HIAF Sample Masses ($\pm 0.05\text{mg}$)	
Sample Name	Mass (mg)
Fe_2O_3	6.1
$\text{PbF}_2+\text{AgF}_2$ 1:1/A	4.7
$\text{PbF}_2+\text{AgF}_2$ 1:1/B	4.2
$\text{PbF}_2+\text{AgF}_2$ 1:2/A	7.4
$\text{PbF}_2+\text{AgF}_2$ 1:2/B	4.0
$\text{PbF}_2+\text{AgF}_2$ 1:5/A	4.1
$\text{PbF}_2+\text{AgF}_2$ 1:5/B	5.1
$\text{PbF}_2+\text{AgF}_2$ 1:10/A	3.0
$\text{PbF}_2+\text{AgF}_2$ 1:10/B	3.0

Table 3: $\text{PbF}_2+\text{AgF}_2$ sample masses alongside Fe_2O_3 sample mass. The 1:10 samples are low in mass as most of the sample was lost since it was smeared and burnt as it was wet.

2.3 Degradation Procedures

2.3.1 $\text{PbF}_2 + \text{AgF}_2$ Sample Preparations

2.3 mg PbF_2 and 9.3 mg AgF_2 were weighed out and mixed. AgF_2 was light and black. Mixing process for this sample resulted in heavy smearing. The mixture was not differentiable and AgF_2 had properties that allowed no possibility of transfer to the cathode. These include it being reactive to air, absorbent to moisture, sticky, and paint-like once in contact with a surface.

To overcome these issues, another method was used and the rest of the samples were prepared as follows. 4.8mg of AgF_2 was directly weighed into a teflon vial, 100 μL of 48% HF was added, and this was transferred into the heating block. After the reaction subsided, 2.5 mg of PbF_2 was weighed into the teflon vial and the addition of 100 μL HF was repeated and then put into the heating block.

2.3.2 $\text{PbF}_2 + \text{SbF}_3$ Sample Preparations

Another fluorinating agent is SbF_3 . Therefore, Sb_2O_3 (BDH Chemicals) was used and

transferred into a Teflon vial. $100 \mu\text{L}$ of 48% HF was added to convert to SbF_3 and then placed into the heating block. 2.8 mg of PbF_2 was weighed and then transferred after the reaction subsided. $100 \mu\text{L}$ of HF was again added and put into the heating block, which formed a embroidered and white crater-like structure overtime. This process was repeated for all the other samples.

2.3.3 Degradation Set Preparation

The $\text{PbF}_2 + \text{AgF}_2$ –1 and $\text{PbF}_2 + \text{AgF}_2$ –5 sample masses were calculated; with them weighing 7.4 mg and 37.3 mg respectively. The $\text{PbF}_2 + \text{AgF}_2$ –1 was pressed, and the $\text{PbF}_2 + \text{AgF}_2$ –5 was used to press 5 samples. The mixtures were prone to heavy smearing and were sticky. A significant amount of mass was either stuck to the crucible or weighing paper and was not transferable, so the measured masses were smaller than the expected 2.5mg PbF_2 + 5.0mg AgF_2 mixture standard.

Mass calculation was done for $\text{PbF}_2 + \text{SbF}_3$ –1 and $\text{PbF}_2 + \text{SbF}_3$ –5, yielding 20.3 mg and 110.8 mg respectively. $\text{PbF}_2 + \text{SbF}_3$ –1 was pressed. 5 samples were pressed with $\text{PbF}_2 + \text{SbF}_3$ –5.

The cathodes were set up in air and in N_2 . The cathodes to be in N_2 were laid out in a small, sealed plastic bag and N_2 was pumped. The rest were laid out exposed to air. Table 4 shows the degradation sample masses.

Degradation Sample Masses ($\pm 0.05\text{mg}$)	
Sample Name	Mass (mg)
PbF₂ + AgF₂ Samples	
PbF ₂ _AgF ₂ _Al_D	3.4
PbF ₂ _AgF ₂ _Al_D/N2	4.8
PbF ₂ _AgF ₂ _SS_D	6.5
PbF ₂ _AgF ₂ _SS_D/N2	5.3
PbF ₂ _AgF ₂ _Cu_D	3.7
PbF ₂ _AgF ₂ _Cu_D/N2	4.4
PbF₂ + SbF₃ Samples	
PbF ₂ _SbF ₃ _Al_D	20.3
PbF ₂ _SbF ₃ _Al_D/N2	15.4
PbF ₂ _SbF ₃ _SS_D	14.9
PbF ₂ _SbF ₃ _SS_D/N2	15.9
PbF ₂ _SbF ₃ _Cu_D	12.5
PbF ₂ _SbF ₃ _Cu_D/N2	14.2

Table 4: Degradation sample masses for $\text{PbF}_2 + \text{AgF}_2$ and $\text{PbF}_2 + \text{SbF}_3$

3. RESULTS

3.1 Carrier Purity Results

–1 and –2 samples were measured at VEGA, a 1 MV accelerator at ANSTO by Dr Michael Hotchkis. The purified samples (–2) were compared with unpurified samples (–1) to see if there was an effect on the isotopic ratio of ^{210}Pb to ^{208}Pb . This is because a purified sample would contain less impurities, which would mean less chance of clusters forming that would have the same mass as ^{210}Pb or ^{208}Pb . All samples were measured in a +2 charge state. Within these, a $^{210}\text{Pb}/^{208}\text{Pb}$ solution (10–11–2) with a known ratio of 1.95E–11 was prepared and also measured. After the AMS measurement, the $^{210}\text{Pb}/^{208}\text{Pb}$ isotopic ratios were calculated and then normalised to the 10^{-11} standard to ensure that all samples were corrected. This correction was done by calculating a normalisation factor, which was given by: normalization = $\frac{\text{measured ratio of } 10-11-2}{1.95\text{E}-11}$. This was calculated to be 1.112.

Isotopic ratios and their uncertainties are compared and their values are shown in Figure 2 and Table 5. Table 5 shows that the $^{210}\text{Pb}/^{208}\text{Pb}$ ratio is higher for the –2 samples than the –1 samples. This is unexpected as a high ratio indicates more ^{210}Pb cps and thus more ^{210}Pb . This means that the –2 samples had more ^{210}Pb , or other molecules of mass 210 amu. A possibility is that the –2 sample procedures introduced contamination.

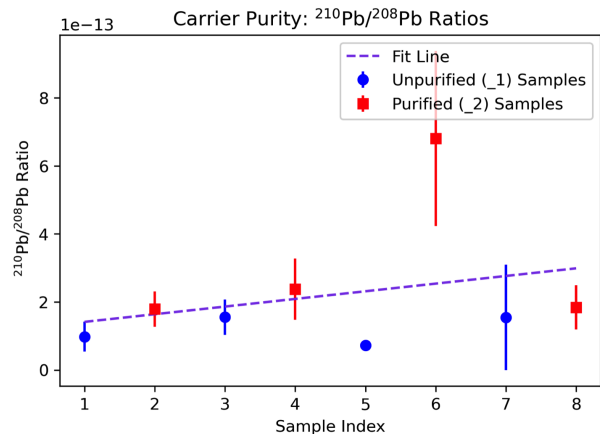


Figure 2: Ratios of $^{210}\text{Pb}/^{208}\text{Pb}$ of –1 and –2 samples

Figure 2 shows that all samples except for the PbF_2 pair are in agreement with their uncer-

tainties. The PbF_2 _1 sample had the lowest ratio and the lowest uncertainties out of the whole and the _2 sample the opposite. This is strange as the _1 was unpurified and was exposed to air. This means that there should be more impurities formed as a result of the moisture, and a decreased performance in AMS as PbF_2 absorbs moisture. This would increase the chance of measuring ^{210}Pb counts, leading to a larger ratio. It's _2 counterpart had the highest value and uncertainty despite going through purification.

Carrier Purity: Propagated Ratios			
Sample Index	210/208 Ratio	Sample Index	210/208 Ratio
1. Pb_20002	9.78E-14 ± _1/A	5. PbF_2	7.19E-14 ± _1/A
2. Pb_20002	1.79E-13 ± _2/A	6. PbF_2	6.81E-13 ± _2/A
3. Pb_20003	1.55E-13 ± _1/A	7. PbO_2	1.55E-13 ± _1/A
4. Pb_20003	2.38E-13 ± _2/A	8. PbO_2	1.84E-13 ± _2/A
			6.50E-14

Table 5: _1 and _2 $^{210}\text{Pb}/^{208}\text{Pb}$ Ratio values as shown to Figure 2. The sample index in Figure 2 corresponds to the sample name.

It is likely that the PbF_2 _2 sample was contaminated. This contamination might have spread to the other _2 samples, which is an explanation as to why their ratios are higher. An interesting note is that the mistaken addition of HCl to $\text{Pb}_\text{20002_1}$ and $\text{Pb}_\text{20003_1}$ samples did not seem to have an impact as they are still close to each other and also go through the best fit line. This means that although 10mL of HCl was introduced, a volume 100 times as much as the HF, significant amount of ^{210}Pb was not introduced.

For purification, it is likely that there are impurities coming together with Pb and forming compounds that go through the columns. A multi-elemental scan using ICP-MS would be beneficial to check what impurities are present in the final samples. Additionally, an ICP-MS scan of the resin, Fe fraction and Pb fraction would also be beneficial before sample preparation as this would give an indication of how effective the resin is and how many impurities were retained

or passed through. Examining with a different resin that can catch a higher number of impurities would be beneficial. This means that the effects of contamination can be minimised, and more impurities can be caught leading to a purer sample. Other AE Resins that are based around NH_2 , NR_2 and NHR could be tried to see if there are less impurities present. AE Resins are made of ST(Styrene) and DVB(Divinylbenzene) copolymers. These polymers are cross-linked through DVB as a cross-linking agent [11]. The degree of cross-linkage can be modified by the percent of DVB. Experimenting with the addition of DVB could lead to an optimal degree of cross-linkage. This would increase the resin's rigidity and hardness, and would effectively stabilise the resin. This might improve the resin's ability to retain and catch impurities.

There is also the possibility of error within the VEGA accelerator. As two samples were made, if the /B samples were tested at a different time, this would prove whether or not there was a systematic error. Uncertainties can be reduced by measuring for longer periods of time. This would give a better indication of whether the samples are in agreement with each other.

3.2 Carrier Efficiency Results

Figures 3 to 5 show the trend of the current over the time of 2000s measured at HIAF. Table 2 shows the integrated current of these samples. This was calculated via the relationship: integrated current = Σ currents $\times \frac{\text{loop time}}{2}$. All $\text{PbF}_2 + \text{AgF}_2$ samples as part of the first HIAF measurements rapidly decreased to low currents, with the 1:5/B and 1:10/A dying halfway through. Figure 4 shows a zoomed in version of the graph. The 1:5/B and 1:10/A immediately plateaued, and the other two rapidly decreased, with the 1:1/A sample fluctuating up and down till a plateau was reached. The currents for 1:2/A, 1:5/B and 1:10/A were all low, and discounting the initial drop, the 1:1/A current was also similar.

This was the opposite of the hypothesis, which predicted that these samples would have the best current output. It is possible that $\text{PbF}_2 + \text{AgF}_2$ as an AMS target is unstable and unpredictable. Past procedures have involved CsF that proved to be unstable and reactive, performing badly in AMS.

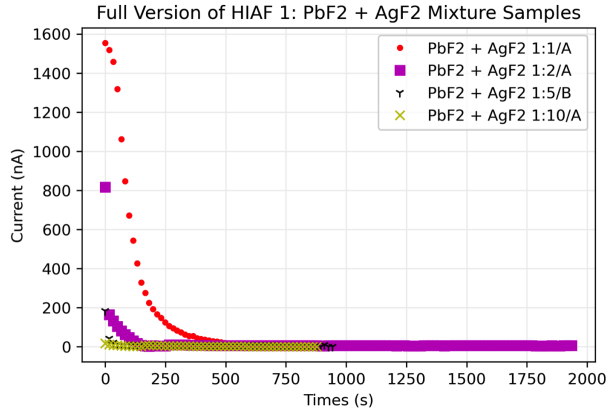


Figure 3: 1st HIAF run of $\text{PbF}_2 + \text{AgF}_2$ mixtures with mainly /A samples. The 1:5/B sample was used as the /A sample was used initially to detect different Pb isotopes when calibrating the accelerator. This figure includes the whole scale of the measurements.

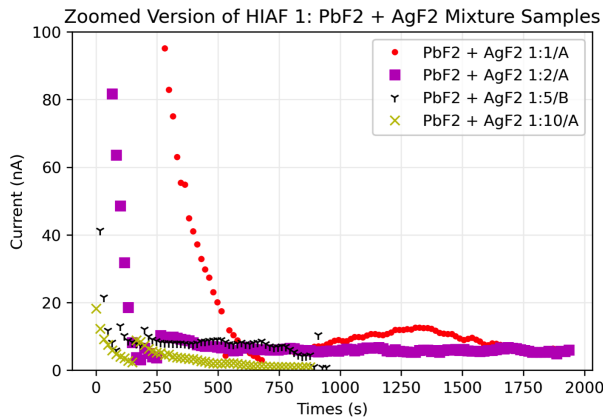


Figure 4: A zoomed in version of Figure 2 showing fluctuations at the low current levels.

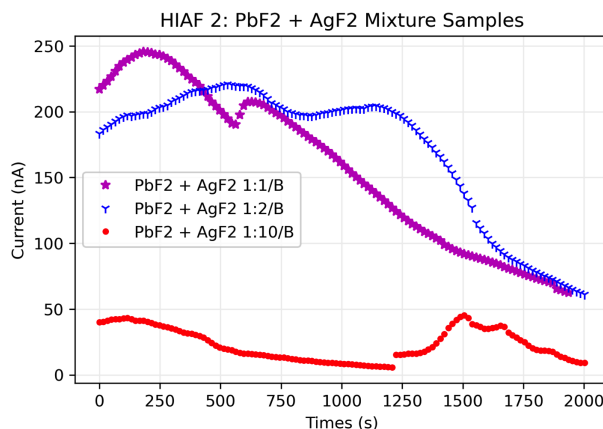


Figure 5: 2nd HIAF run of $\text{PbF}_2 + \text{AgF}_2$ mixtures with /B counterparts.

HIAF 1 and 2 Propagated Data	
Sample Name	Integrated Current [C]
PbF2+AgF2 1:1/A	2.00E-04
PbF2+AgF2 1:2/A	3.46E-05
PbF2+AgF2 1:5/B	1.07E-05
PbF2+AgF2 1:10/A	3.12E-06
PbF2+AgF2 1:1/B	3.01E-04
PbF2+AgF2 1:2/B	3.36E-04
PbF2+AgF2 1:10/B	4.52E-05

Table 6: Integrated Currents of $\text{PbF}_2 + \text{AgF}_2$ samples run through HIAF

Another possibility is that human error was introduced. This could come from setting the wrong values for the accelerator parameters or leaving the sample in for too long before the measurement period.

To test these cases, the /B samples were measured. These resulted in much better current outputs. The 1:1/B and the 1:2/B were equal in magnitude, and were also an order of magnitude higher than the 1:2/A, 1:5/B and 1:10/A. Despite this, these samples lacked stability. Figure 5 shows no linear trend or slow eventual decrease, but rather spontaneous fluctuations at random times. This adds a degree of unpredictability to these samples, which could possibly mean the sample is unstable and behaves sporadically as an AMS target. As F atoms present in the sample, there is a higher chance of lead-fluorine ions such as PbF^- or PbF_4^- being formed. These could then produce side reactions with Cs^+ or other molecules and cause the sample to behave unpredictably. Additionally, although predicted to have the best current output, the $\text{PbF}_2 + \text{Ag}$ samples (prepared by M. Webber) had more stable and higher current outputs, with the 1:1 ratio being the best. This is best used as AMS target compared to $\text{PbF}_2 + \text{AgF}_2$.

A possible conclusion for the performance in Figure's 3 and 4 is that the ioniser current was too high and there was too much caesium. A high ioniser current causes the temperature of caesium to rise. This sputtered the sample too quickly, and during measurement, there was close to none left. The lack of current for the 1:10 samples compared to the rest can be attributed to the lack of sample material as the sample was burnt and infused with weighing paper. This could have also played an effect as to why the 1:10/A was consumed quicker and the 1:10/B output was an

order of magnitude lower than the other /B samples.

Figure 6 shows the sputtering of the $\text{PbF}_2 + \text{AgF}$ 1:10_1 sample for efficiency with an exponential and linear fit fitted around the marked area. The efficiency was calculated by combining all $\text{BF}_2 + \text{AgF}$ 1:10_1 measurements and then finding the ratio of extracted Pb ions to the total mass in the original sample.

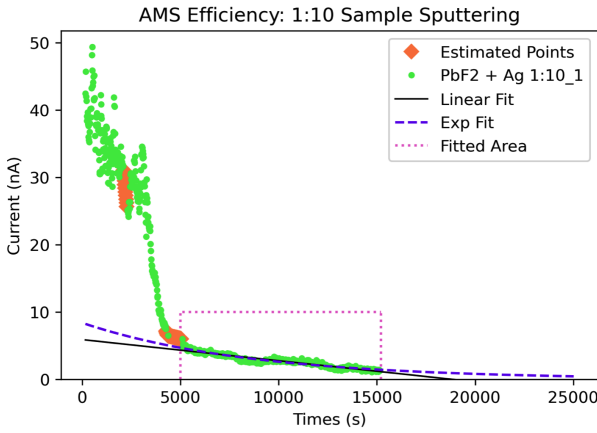


Figure 6: Overall sputtering of $\text{PbF}_2 + \text{AgF}$ 1:10_1

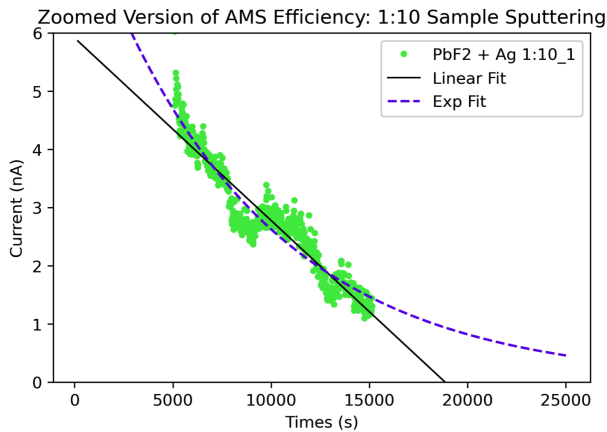


Figure 7: Zoomed in version of fit area showing the difference between exponential and linear fit.

$$\% \text{ efficiency} = \frac{\text{total ions extracted}}{\text{total Pb atoms in sample}}.$$

Given a mass of 1.0mg, there were $1.2\text{E}+18$ total atoms, as calculated by:

$$\text{sample mass} \times {}^{208}\text{Pb abundance} \times 1 \text{ mol} \over \text{amu of } \text{PbF}_2$$

The extracted material was found by summing all the currents and adding the expected value with the exponential and linear fits till

the sample ended. Where there were gaps in the current values, a linear fit between the gaps was used to interpolate between points. These are the estimated points (shown in Figure 6). Although in Figure 6 both fits seem identical, Figure 7 shows that in the fitted area, there is a slight difference and the exponential fits better. The chi-squared values also indicate this. The exponential fit chi-squared was 18.45 and the linear fit was 18.90. The linear fit resulted in an efficiency of 0.077%, whereas the exponential fit gave 0.081%. The linear fit was stopped at 0 nA, but as the exponential was estimated to stop at 0.45 nA as further forecasting does not impact the efficiency calculation.

Improvements to the efficiency calculation include sputtering to completion and sputtering multiple samples. These could then be compared with each other and uncertainties can be quantified. A WLS regression can be performed and a better indication as to how the sample behaves overtime can be attained. This gives a better measurement of the beam efficiency. A more stable and predictable AMS target would also benefit improving the beam efficiency. This would make it easier to fit and forecast.

3.3 Degradation Results

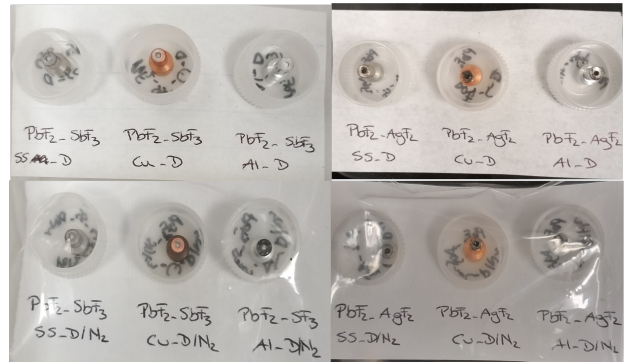


Figure 8: Initial observations of degradation samples

Figure 8 shows the degradation samples when first prepared, and Figure 9 shows them 26 days apart from being exposed. No significant change was seen between this time period. No cathode surfaces were changed since first observed.

Future work would ensure that while pressing, pressure is applied to the cathode. This lessens the likelihood of the sample spilling on the cathode surface. Spills on the cathode surface can make actual degradation unidentifiable. This

happened for some of the samples, thus making the results for these samples inconclusive as there could have been degradation.

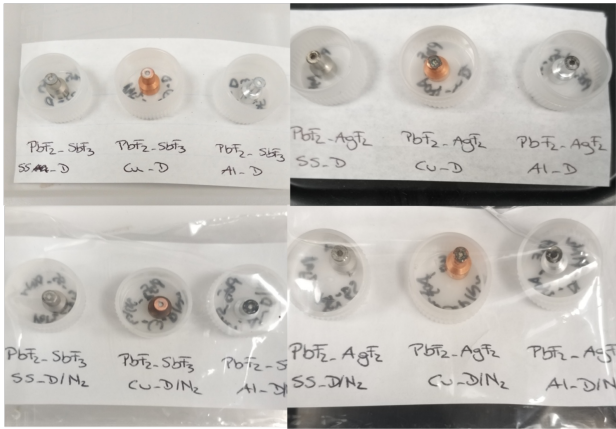


Figure 9: Final observations of degradation samples

Improvements would include methods to clean the cathode surface in such a way to remove the spill but not affect any potential degradation. Further change might be observed if left for 8-10 weeks instead.

4. CONCLUSION

The purpose of this project to characterise the behaviour of ^{210}Pb through measuring ^{208}Pb and ^{210}Pb ion output, efficiency and degradation was achieved using primarily AMS. The Pb ion output tests from ANSTO resulted in unpurified samples having lower $^{210}\text{Pb}/^{208}\text{Pb}$ isotopic ratios than the purified samples likely due to the purified samples being contaminated. Samples of $\text{PbF}_2+\text{AgF}_2$ that were tested for efficiency showed that they were sporadic and unpredictable as an AMS target, but did give satisfactory current outputs. The efficiency of the beam was calculated to be 0.081% using exponential forecasting from the sputtering of the $\text{PbF}_2+\text{AgF}_2$ 1:10_1 sample. Degradation samples yielded inconclusive results. There was no observed change in $\text{PbF}_2+\text{AgF}_2$ or $\text{PbF}_2+\text{SbF}_2$ samples, and more time was needed to make an accurate conclusion. Further work and improvements would involve new ideas and research to help improve AMS facilities and procedures for the purpose of making carriers and examining ^{210}Pb .

-
- [1] Tarun Biswas. Spiral galaxy rotation curves without dark matter or mond – two conjectures, 2018.
 - [2] M. Antonello, E. Barberio, T. Baroncelli, J. Benziger, and L.J. Bignell et al. Monte carlo simulation of the sabre pop background. *Astroparticle Physics*, 106:1–9, 2019.
 - [3] R. Bernabei, P. Belli, A. Bussolotti, and F. Cappella et al. The dama project: Achievements, implications and perspectives. *Progress in Particle and Nuclear Physics*, 114:103810, 2020.
 - [4] K Garrett and G Duda. Dark matter: A primer. *Advances in Astronomy*, 2011:1–22, 2011.
 - [5] M. Antonello, E. Barberio, T. Baroncelli, and J. Benziger et al. The sabre project and the sabre proof-of-principle. *The European Physical Journal C*, 79(4), Apr 2019.
 - [6] Madeleine J. Zurowski, Elisabetta Barberio, and Giorgio Busoni. Inelastic dark matter and the sabre experiment. *Journal of Cosmology and Astroparticle Physics*, 2020(12):014–014, Dec 2020.
 - [7] M. Antonello, I. J. Arnquist, E. Barberio, and T. Baroncelli et al. Characterization of sabre crystal nai-33 with direct underground counting. *The European Physical Journal C*, 81(4), Apr 2021.
 - [8] R. Bernabei, P. Belli, F. Cappella, and R. Cerulli et al. New results from dama/libra. *The European Physical Journal C*, 67(1–2):39–49, Mar 2010.
 - [9] R. Bernabei, P. Belli, V. Caracciolo, and R. Cerulli et al. The dark matter: Dama/libra and its perspectives, 2021.
 - [10] A. Sookdeo, R. J. Cornett, X.-L. Zhao, and C. R. J. Charles et al. Measuring ^{210}pb by accelerator mass spectrometry: a study of isobaric interferences of 204 , 205 , 208 pb and 210 pb. *Rapid Communications in Mass Spectrometry*, 30(7):867–872, February 2016.
 - [11] S Jiang, X Sun, L Ling, and S Wang et al. Preparation and characterization of (st-DVB-MAA) ion exchange resins. In *AIP Conference Proceedings*. Author(s), 2017.